of heteroclusters, the relative reaction rate *increases* as a function of cluster size. This may be due to a reduction in the stability of the heterocluster ion with cluster size (in contrast to the situation for homoclusters).

(6) In the case of heterocluster ions it is possible for the initial ion to abstract a hydrogen from each of two different molecules. We find that the branching ratios depend in a statistical manner on the M/A ratio, i.e., the composition of the cluster. Increasing the proportion of one molecule increases the relative rate of formation of the product resulting from that molecule.

(7) The protonated cluster ion can undergo additional (possibly termolecular) ion-molecule reactions which can eliminate either HX or CH_4. In addition, for the case of dimethyl ether (and CH_3F[29]), novel termolecular reactions also occur, producing new product ions. It is speculated that they arise because of the solvated environment of the cluster, the exothermic nature of the precursor reactions, and the very stable ion products formed.

Acknowledgment. This research has been supported by NSF Grant CHE83-16205, hereby gratefully acknowledged. The authors thank T. J. Curtiss, S. R. Gandhi, and Qixun Xu for their work in connection with the design and construction of the molecular beam machine. We also thank Prof. Tomas Baer for a useful suggestion concerning the stability of dimer ions.

Solvent Bandwidth Dependence and Band Asymmetry Features of Charge-Transfer Transitions in *N*-Pyridinium Phenolates

A. M. Kjaer and J. Ulstrup*

Contribution from the Chemistry Department A, Building 207, The Technical University of Denmark, 2800 Lyngby, Denmark. *Received August 25, 1986*

Abstract: We have investigated the shape of the solvatochromic absorption band for "Betaine-26" 2,4,6-triphenyl-*N*-(di-*tert*-butyl-4-hydroxyphenyl)pyridinium ion in a range of polar, apolar, protic, and aprotic solvents. Multiphonon band theory, including both molecular modes and a vibrationally dispersive solvent, indicates that the solvents fall in three categories: (1) The bandshape for polar, aprotic solvents is well reproduced by that for a structureless continuous dielectric and a single high-frequency molecular mode. Solvent broadening correlates with $\epsilon_o^{-1} - \epsilon_s^{-1}$, ϵ_o being the optical and ϵ_s the static dielectric constant. The molecular frequency, Ω_c, and displacement, Δ_c, are not very solvent dependent, emphasizing their molecular character, and the value $\Omega_c \approx 1600$ cm^{-1} suggests that C-O, C-N, and C-C stretching is involved. (2) Bands for apolar, aprotic solvents correspond to the same model. Ω_c and Δ_c are again not very solvent dependent and coincide with the values for polar aprotic solvents. The solvent broadening is solvent independent, and wider than that for a structureless dielectric. This points to multipolar, dispersive, pressure, or pseudopotential forces as coupling mechanisms. (3) The bandshape for normal alcohols can only be reproduced by a model resting on two molecular modes and a vibrational high-frequency solvent "tail". Broadening, asymmetry, molecular frequencies, and deuterium isotope effects trace the protic solvent spectral entanglement to coupling between betaine-26 and a local mode group with features of both O-H stretching and bending and of librational solvent motion.

I. Introduction

Molecular solute charge transfer transitions between donor (ground state) and acceptor (excited state) orbitals exposed to the external solvent are strongly coupled to environmental polarization fluctuations. Such systems are, for example, donor-acceptor complexes,[1-3] ion pairs,[4-14] mixed-valence compounds,[15-24] and certain large organic aromatic molecules.[25-33] Most directly, and least dependent on particular solvent models, strong coupling is reflected by time-resolved fluorescence where an excited state potential surface is strongly displaced relative to the ground state surface along a suitably constructed set of solvent nuclear modes and relaxes along these coordinates subsequent to excitation, the relaxation time being correlated to the solvent dielectric relaxation times.[29-33]

Strong solute-solvent coupling charge transfer absorption band profiles are also characterized by solvent-induced band maximum, bandwidth, and bandshape features. With few exceptions such effects have been ascribed, either to inhomogeneous broadening or to specific molecular effects such as hydrogen bonding, handled largely in a qualitative fashion. Dynamic solvent effects and solute

(1) Briegleb, G. *Electronen-Donator-Akceptor-Komplekse*; Springer-Verlag: Berlin, 1961.
(2) *Molecular Complexes*; Foster, R., Ed.; Elek Science: London, 1974; Vol. 1 and 2.
(3) Foster, R. *J. Phys. Chem.* **1984**, *84*, 2135.
(4) Kosower, E. M. *J. Am. Chem. Soc.* **1958**, *80*, 3253.
(5) Kosower, E. M.; Skorcz, J. A. *J. Am. Chem. Soc.* **1960**, *82*, 2195.
(6) Mackay, R. A.; Landolph, J. R.; Poziomek, E. J. *J. Am. Chem. Soc.* **1971**, *93*, 5026.
(7) Dance, I. G.; Solstad, P. S. *J. Am. Chem. Soc.* **1969**, *91*, 7256.
(8) Nakahara, A.; Wang, J. H. *J. Phys. Chem.* **1963**, *67*, 496.
(9) MacFarlane, A. J.; Williams, R. J. P. *J. Chem. Soc., Dalton Trans.* **1969**, 1517.
(10) (a) Toma, H. E. *Can. J. Chem.* **1979**, *57*, 2079. (b) Toma, H. E. *J. Chem. Soc., Dalton Trans.* **1980**, 471.
(11) Curtiss, J. C.; Sullivan, B.; Meyer, T. J. *Inorg. Chem.* **1980**, *19*, 3833.
(12) Curtiss, J. C.; Meyer, T. J. *Inorg. Chem.* **1982**, *21*, 1562.
(13) Kristjansson, I.; Ulstrup, J. *Chem. Scr.* **1985**, *25*, 58.
(14) Kjaer, A. M.; Kristjánsson, I.; Ulstrup, J. *J. Electroanal. Chem.* **1986**, *204*, 45.
(15) (a) Hush, N. S. *Prog. Inorg. Chem.* **1967**, *8*, 391. (b) Hush, N. S. *Electrochim. Acta* **1968**, *13*, 1005.
(16) Tom, G.; Creutz, C.; Taube, H. *J. Am. Chem. Soc.* **1974**, *96*, 7828.
(17) (a) Taube, H. *Ber. Bunsenges. Phys. Chem.* **1972**, *76*, 964. (b) Taube, H. *Adv. Chem. Ser.* **1977**, *162*, 127. (c) Taube, H. In *Tunneling in Biological Systems*; Chance, B., DeVault, D. C., Frauenfelder, H., Marcus, R. A., Schrieffer, J. R., Sutin, N., Eds.; Academic: New York, 1979; p 173.
(18) Meyer, T. J. *Acc. Chem. Res.* **1978**, *11*, 94.
(19) Powers, M. J.; Salomon, D. J.; Callahan, R. J.; Meyer, T. J. *J. Am. Chem. Soc.* **1976**, *98*, 6731.
(20) (a) Powers, M. J.; Meyer, T. J. *J. Am. Chem. Soc.* **1978**, *100*, 4393. (b) Powers, M. J.; Meyer, T. J. *J. Am. Chem. Soc.* **1980**, *102*, 1289.
(21) German, E. D.; Kuznetsov, A. M. *Electrochim. Acta* **1981**, *26*, 1595.
(22) Creutz, C. *Prog. Inorg. Chem.* **1983**, *30*, 1.
(23) (a) Ludi, A. In *Mixed-Valence Compounds*; Brown, D. B., Ed.; Reidel: Dordrecht, 1980, p 25. (b) Joss, J.; Bürgi, H. B.; Ludi, A. *Inorg. Chem.* **1985**, *24*, 949 and references there.
(24) Kornyshev, A. A.; Ulstrup, J. *Chem. Phys. Lett.* **1986**, *126*, 74.
(25) Dimroth, K.; Arnoldy, G.; von Eichen, S.; Schiffer, G. *Ann. Chem.* **1957**, *604*, 221.
(26) Dimroth, K.; Reichardt, C.; Siepmann, T.; Bohlmann, F. *Ann. Chem.* **1963**, *661*, 1.
(27) Dimroth, K.; Reichardt, C.; Schwieg, A. *Ann. Chem.* **1963**, *669*, 95.
(28) Reichardt, C. *Angew. Chem.* **1965**, *77*, 30.
(29) Grabowski, Z.; Rothiewicz, K.; Siemiarczuk, A.; Cowley, D. J.; Baumann, W. *Nouv. J. Chim.* **1979**, *3*, 443.
(30) Pettig, W. *J. Lumin.* **1980**, *26*, 21.
(31) Wang, Y.; Eisenthal, K. B. *J. Chem. Phys.* **1982**, *77*, 6076.
(32) (a) Kosower, E. M.; Huppert, D. *Chem. Phys. Lett.* **1983**, *96*, 443. (b) Giniger, R.; Huppert, D.; Kosower, E. M. *Chem. Phys. Lett.* **1985**, *118*, 240.
(33) Villayes, A. A.; Boeglin, A.; Lin, S. H. *J. Chem. Phys.* **1985**, *82*, 4044.

0002-7863/87/1509-1934$01.50/0

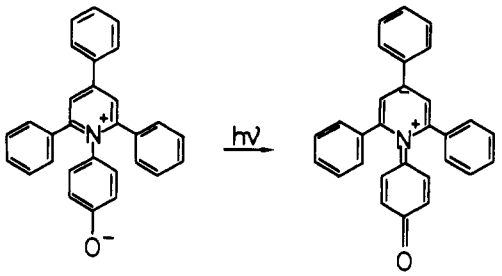

Figure 1. Schematic view of the solvatochromic charge transfer transition in betaines[28] (shown for "betaine-1"[26]).

molecular charge transfer transitions resting on potential surfaces spanned by solvent nuclear coordinates have received much less attention.

Following the introduction of the concept of mixed-valence transitions[34] and the observation by Hush[15] that where thermal intermolecular electron transfer occurs there must also be a corresponding optical transition, a range of investigations of solvent effects on intervalence transitions in mixed-valence bi- and trinuclear transition metal complexes were reported.[16-20,22,23] Their interpretation rested on a dynamic view of the solvent and inertial polarization shift as a crucial origin of observed near-infrared intervalence absorption. In some cases the absorption maximum energy displays correlations with the solvent dielectric parameter $\epsilon_0^{-1} - \epsilon_s^{-1}$,[16-20,22] as for a "classical", structureless dielectric, where ϵ_0 is the optical and ϵ_s the static dielectric constant and with a charge transfer distance characteristic of the geometric representation of the absorbing molecule. In other cases the correlations fail, and more elaborate solvent representations,[21,24] for example, involving nonlocal dielectric theory and solvent vibrational frequency dispersion,[24,35] are needed. Such representations incorporate solvent structural features and clearly go beyond structureless continuum models, which have so far been almost the sole theoretical frame for the reported investigations.

In this work we attend in greater detail and in the light of more recent achievements of electron transfer theory[36-42] to the bandshape of optical charge transfer transitions involving extensive electronic rearrangement analogous to chemical electron transfer. In particular we shall emphasize the role of solvent vibrational frequency dispersion as reflected in the frequency-dependent dielectric permittivity. In addition we shall note the possible variation in the electronic transition dipole with the instantaneous inertial polarization imposing bandshape modifications relative to the pure Condon bandshapes. We shall illustrate the formalism by analysis of the detailed bandshape of the "solvatochromic" charge transfer band of "betaine-26", i.e., 2,4,6-triphenyl-*N*-(3,5-di-*tert*-butyl-4-hydroxyphenyl)pyridinium ion,[26,28] in a wide range of solvents. This compound is representative of a broad class of compounds which possess an exceedingly solvent sensitive visible or near-infrared charge transfer transition which has been used as a basis for the empirical solvent E_T polarity scale.[25-28] The transition can be roughly ascribed to intramolecular electron transfer from the phenolate group in the "lower" ring to the carbon atom in the "top" ring in the p-position relative to the pyridinium nitrogen atom (Figure 1).[28] In contrast to the bands for a range of other betaines, the betaine-26 band is well separated from other bands. It is furthermore quite strongly asymmetric with a slower fall-off on the high-frequency side of the maximum, indicative of reorganization in molecular high-frequency nuclear modes in addition to those of the solvent. It is finally possible to vary the solvent over much wider ranges of the dynamic solvent polarity parameter $\epsilon_0^{-1} - \epsilon_s^{-1}$ than for mixed-valence complexes. The solvent broadening appears well represented by the pattern for structureless dielectrics for aprotic solvents in roughly the same range of $\epsilon_0^{-1} - \epsilon_s^{-1}$ as for some intervalence transitions, but a more entangled picture emerges outside this range and for hydroxylic solvents in particular.

II. Experimental Section

Materials. 2,4,6-triphenyl-*N*-(3,5-di-*tert*-butyl-4-hydroxyphenyl)-pyridinium perchlorate (betaine-26[25,26]) was prepared by combining the "upper" part, i.e., 2,4,6-triphenylpyrylium perchlorate, with the primary amino group in the "lower" part, i.e., 2,6-di-*tert*-butyl-4-aminophenol. These two constituents were obtained by separate preparations. The scheme is a general route toward a wide variety of *N*-pyridinium compounds,[42] and the following procedures, slightly modified from the ones reported in ref 25-27, 43, and 44, were used.

2,4,6-Triphenylpyryliumtetrachloroferrate(III).[44] Benzylideneacetophenone (15.6 g) and 9.0 g of acetophenone were dissolved in 115 mL of carbon disulfide and 36.5 g of anhydrous ferric chloride was added with cooling and stirring. The ferric chloride was BDH laboratory quality. Fresh samples were used, but sublimination was found to be unnecessary. Acetanhydride (25 mL) was added in small portions with stirring and the mixture refluxed for 2 h. Orange crystals precipitated after cooling and were isolated and washed several times with glacial acetic acid and ether. Yield, 19.8 g; mp 275-277 °C (lit.[25] mp 275 °C).

2,4,6-Triphenylpyrylium Perchlorate.[25-27,44] Five grams of the tetrachloroferrate(III) salt were dissolved in 20 mL of glacial acetic acid and 400 mL of water. The yellow perchlorate was obtained by adding 10 mL of 70% perchloric acid, filtering and washing with water: mp 248-249 °C as reported in ref 25.

2,6-Di-*tert*-butyl-4-aminophenyl[25-27] was prepared from 2,6-di-*tert*-butylbenzoquinone, conversion of this compound to the analogous 4-nitrosophenol, and reduction of the nitroso group to the amino form by dithionite.

2,6-Di-*tert*-butylbenzoquinone.[41] This compound was prepared by oxidation of 2,6-di-*tert*-butyl-*p*-cresol by chromic anhydride as in ref 43. The final washed and dried ether fraction was vacuum distilled and the fraction at 89-95 °C (0.20 mmHg) collected. The yield of the orange solid was 10.8 g or 16.2%.

2,6-Di-*tert*-butyl-4-nitrosophenol. The quinone was converted to the nitrosophenol by reduction with hydroxylamine as in ref 43. The product was recrystallized from carbon tetrachloride. The melting point (230-231 °C) and molar extinction coefficient (2.04×10^4 dm^3 mol^{-1} cm^{-1}) were both somewhat higher than reported[43] (211 °C and 1.78×10^4 dm^3 mol^{-1} cm^{-1}, respectively).

2,6-Di-*tert*-butyl-4-aminophenol.[44] The nitroso compound (2.55 g) dissolved in 10 mL of aqueous 5% sodium hydroxide was heated to 45-60 °C and 4.57 g of sodium dithionite slowly added. In previous reports[25] this reduction was effected by dihydrogen and Raney nickel. The solution was diluted with water to 20 mL, cooled, and filtered. The cream-colored crystals were washed with water and immediately used for coupling with the pyrylium salt. The crystals rapidly turn red on standing: mp 109 °C (sharp) (lit.[26] mp 108-112 °C).

2,4,6-Triphenyl-*N*-(3,5-di-*tert*-butyl-4-hydroxyphenyl)pyridium Perchlorate.[25] This compound was obtained from 2,4,6-triphenylpyrylium perchlorate and 2,6-di-*tert*-butyl-4-aminophenol by the procedure in ref 25. The crystals were recrystallized from ethanol: mp 277-278 °C as reported in ref 25.

The betaine was liberated and recrystallized also by the procedure in ref 25 and kept in a desiccator over solid NaOH: mp 266-268 °C (lit. 266-276 °C).

Solvents and Other Reagents. Millipore water (4-Housing Milli-Q system) and analaR grade organic solvents were used. Organic solvents were dried by molecular sieves (Union Carbide, 4A) for 24 h and further purified on a basic alumina column (Merck, Aktivitätsstufe 1). Purifi-

(34) *Mixed-Valence Compounds*; Brown, D. B., Ed.; Reidel: Dordrecht, 1980.
(35) (a) Kornyshev, A. A. *Electrochim. Acta* **1981**, *26*, 1. (b) In *The Chemical Physics of Solvation*, Part A; Dogonadze, R. R., Kálmán, E., Kornyshev, A. A., Ulstrup, J., Eds.; Elsevier: Amsterdam, 1985; Chapter 3.
(36) Ovchinnikov, A. A.; Ovchinnikov, M. Ya. *Zh. Eksp. Teor. Fiz.* **1969**, *56*, 1278.
(37) (a) Dogonadze, R. R.; Kuznetsov, A. M. *Elektrokhimiya* **1971**, *7*, 763. (b) Dogonadze, R. R.; Kuznetsov, A. M. *Physical Chemistry. Kinetics*; VINITI: Moscow, 1973. Dogonadze, R. R.; Kuznetsov, A. M. *Prog. Surf. Sci.* **1975**, *6*, 1.
(38) Dogonadze, R. R.; Kuznetsov, A. M.; Vorotyntsev, M. A. *Dokl. Akad. Nauk SSSR, Ser. Fiz. Khim.* **1970**, *195*, 1135.
(39) Dogonadze, R. R.; Kuznetsov, A. M.; Vorotyntsev, M. N.; Zaqaraya, M. G. *J. Electroanal. Chem.* **1977**, *75*, 315.
(40) Itskovitch, E. M.; Kuznetsov, A. M.; Ulstrup, J. *Chem. Phys.* **1981**, *58*, 335.
(41) Dogonadze, R. R.; Itskovitch, E. M.; Kuznetsov, A. M.; Vorotyntsev, M. A. *J. Phys. Chem.* **1975**, *75*, 2827.
(42) Itskovitch, E. M.; Ulstrup, J.; Vorotyntsev, M. A. In *The Chemical Physics of Solvation*; Part B; Dogonadze, R. R., Kálmán, E., Kornyshev, A. A., Ulstrup, J., Eds.; Elsevier: Amsterdam, 1986; p 223.
(43) Vaughan, W. R.; Finch, G. K. *J. Org. Chem.* **1956**, *21*, 1201.
(44) Dimroth, K. *Angew. Chem.* **1960**, *72*, 331.

cation was necessary in most cases, as betaines are preferentially solvated by hydroxylic solvents and the spectral pattern disturbed by small amounts of acidic and hydroxylic impurities. Acetone and carbon disulfide decompose by contact with the alumina column, and these solvents were only purified by drying over molecular sieves. All other reagents were analaR grade or highest grade quality available.

Betaine solutions, on which spectral recording was undertaken, contained about 1.8×10^{-3} mol dm^{-3} sodium methanolate to avoid hydrogen bonding and spectral blue-shifts from acidic impurities. Sodium methanolate (for methanol solutions in concentrations up to 9×10^{-3} mol dm^{-3}) did not seem to affect the spectral pattern which generally followed that of literature reports.[25,28] Sodium methanolate is insoluble in most apolar solvents, but a small amount of the solid was still kept in contact with the solutions.

Spectral Recordings. Spectra were recorded on a Varian 2300 spectrophotometer with use of QS or Infrasil cells with light path lengths from 1.0 to 10.0 mm. On-line spectral data were collected in a microprocessor unit constructed by Dr. C. E. Foverskov at this department. This unit was connected to the spectrophotometer by an IEEE-488 interface and the data processed by the University Computing Centre with an IBM 3033 computer and the VM/CMS interacting system.

The direct on-line base-line corrected data were handled by least-squares fitting of theoretical bandshape expressions to the data by means of a rather versatile program, "MINI", developed at this department. Up to 20 parameters can in principle be fitted to a base of up to 400 data points, but only five parameters were usually extracted from the data in the present work.

III. Charge-Transfer Bandshapes in the Solute–Solvent Strong-Coupling Limit

We provide first a few elements of a formalism appropriate for extraction of the electronic–vibrational coupling parameters (the solvent reorganization free energy, and the molecular nuclear coordinate displacements and vibrational frequencies) for the betaine-26 charge-transfer band. This formalism rests on the view that electronic–vibrational coupling is what dominates the bandshape features. It differs from most commonly applied approaches to mixed-valence and ion-pair transitions by incorporating both the "linear" continuous solvent and molecular modes and by allowing for vibrational frequency and spatial dispersion in the solvent coupling. In addition, although we provide the bandshape expressions within a Condon scheme, it is still within the frame of the formalism to incorporate as well inertial solvent polarization modulation of this quantity as non-Condon effects, both of which can be important for "long-range" electron transfer.[45-47]

1. Coupling Soley to a Broadly Frequency Dispersive Solvent. We refer to ref 39–42 and literature quoted there for a detailed exposition of the formalism. If at first we consider coupling to the solvent only, and disregard "internal field corrections", the molar extinction coefficient at the incoming light frequency, ν, is[42]

$$\varkappa_{eg}(\nu) = \frac{2\pi}{(\ln 10)(3c)} h\nu \frac{\beta}{\hbar} |M_{eg}|^2 K(\nu) \tag{1}$$

where c is the light velocity in the solvent, h is Planck's constant, $\hbar = h/2\pi$, M_{eg} is the transition dipole matrix element, and $\beta = (k_B T)^{-1}$, k_B being Boltzmann's constant and T the temperature. The bandshape function $K(\nu)$ now depends rather crucially on the solute–solvent coupling pattern and in particular whether the coupling is "weak" or "broad". We assume that strong-coupling, broad-resonance dispersion limits prevail. This is always representative of charge transfer in liquids and corresponds to the condition

$$\left(\frac{E_s}{\hbar\omega_m}\right)\left(\frac{\Gamma}{\omega_m}\right) \gg 1 \tag{2}$$

where ω_m is the appropriate center of the distribution, Γ is its width, and E_s is the solvent reorganization free energy (cf. below), which is a measure of the "coupling strength".

The band is Gaussian near the maximum in this limit

$$K(\nu) = \frac{2\sqrt{\pi}}{\beta\Delta_s} \exp\left[-\frac{(h\nu - h\nu_m)^2}{\Delta_s^2}\right] \tag{3}$$

The maximum, $h\nu_m$, is at $h\nu_m = E_s + \Delta F_o$, where ΔF_o is the free energy gap between the ground and excited states, while the band width, Δ_s, is determined by the solvent dispersion, i.e., essentially by the dielectric induction difference between the ground and excited states, $\Delta\vec{D}_o(\vec{r})$, and the frequency-dispersive dielectric permittivity, $\epsilon(\omega)$. The explicit form of Δ_s is

$$\Delta_s = \sqrt{2E_s k_B T}\left[\int_0^{\omega_c} f(\omega) \coth(\tfrac{1}{2}\beta\hbar\omega)\, d\omega\right]^{1/2};$$
$$f(\omega) = \frac{\beta}{2\pi^2} \frac{\mathrm{Im}\epsilon(\omega)}{|\epsilon(\omega)|^2} \int d\vec{r}\, [\Delta\vec{D}_o(\vec{r})]^2 \tag{4}$$

where $\mathrm{Im}\epsilon(\omega)$ is the imaginary part of $\epsilon(\omega)$ and ω_c a cut-off frequency to account for transparency regions in the solvent vibrational spectrum. $f(\omega)$ is a "reorganization free energy density", i.e., $f(\omega)$ is related to the overall reorganization free energy by

$$E_s = \frac{1}{\beta}\int_0^{\omega_c} \frac{d\omega}{\omega} f(\omega) \tag{5}$$

The character of $f(\omega)$, i.e., its functional dependence on the frequency ω and temperature, is what determines the spectral band features and their temperature dependence. Suitable representations of $f(\omega)$ are the Debye[48]

$$f_D(\omega) = \frac{\beta}{2\pi^2}(\epsilon_{inf}^{-1} - \epsilon_s^{-1}) \frac{\tau_D}{1 + \omega^2\tau_D^2} \int [\Delta\vec{D}_o(\vec{r})]^2\, d\vec{r};$$
$$\tau_D = \frac{\epsilon_{int}}{\epsilon_s}\tau_D^0 \tag{6}$$

and resonance[48]

$$f_R(\omega) = \frac{\beta}{2\pi^2}\frac{\Gamma_R}{2\Omega_R}(\Omega_R^2 + \Gamma_R^2) \times$$
$$\left[\frac{1}{(\omega - \Omega_R)^2 + \Gamma_R^2} - \frac{1}{(\omega + \Omega_R)^2 + \Gamma_R^2}\right] \int [\Delta\vec{D}_o(\vec{r})]^2\, d\vec{r} \tag{7}$$

dispersions. The former represents thermally activated rotational motion of solvent clusters with the relaxation time τ_D^0, and the latter represents damped elastic displacement with the frequency Ω_R and damping coefficient Γ_R. ϵ_{int} is the real dielectric constant on the high-frequency side of the appropriate vibrational absorption band. In the following we shall not consider separate absorption bands and identify ϵ_{int} by the optical dielectric constant ϵ_o.

In general terms, i.e., independently of the particular form of $\epsilon(\omega)$, ϵ_o and ϵ_s are related to $\epsilon(\omega)$ by

$$\epsilon_o^{-1} - \epsilon_s^{-1} = \frac{2}{\pi}\int_0^{\infty} \frac{d\omega}{\omega} \frac{\mathrm{Im}\epsilon(\omega)}{|\epsilon(\omega)|^2} \tag{8}$$

E_s then also takes the following form, well known from polaron,[49] radiationless electronic transition,[50] and electron-transfer theory[36-39,51]

$$E_s = \frac{1}{8\pi}(\epsilon_o^{-1} - \epsilon_s^{-1}) \int d\vec{r}\, [\Delta\vec{D}_o(\vec{r})]^2 \tag{9}$$

It is, however, essential to maintain the band width form in eq 4 at low temperatures or when the solvent has high-frequency

(45) Kuznetsov, A. M. *Nouv. J. Chem.* **1981**, *5*, 427.
(46) (a) Kuznetsov, A. M.; Ulstrup, J. *Faraday Discuss. Chem. Soc.* **1982**, *74*, 31. (b) *Phys. Status. Solidi B* **1982**, *114*, 673. (c) *Chem. Phys. Lett.* **1982**, *93*, 121.
(47) Kuznetsov, A. M.; Ulstrup, J. *Proc. 19th Jerusalem Symp. on Tunnelling*; Jortner, J., Pullman, B., Eds.; Reidel: Dordrecht; in press.
(48) Fröhlich, H. A. *Theory of Dielectrics* 2nd ed.; Clarendon: Oxford, 1958.
(49) Pekar, S. I. *Untersuchungen über die Elektronentheorie der Kristalle*; Akademie Verlag: Berlin, 1954.
(50) (a) Kubo, R. *Phys. Rev.* **1952**, *86*, 929. (b) Kubo, R.; Toyozawa, Y. *Prog. Theor. Phys.* **1955**, *13*, 160.
(51) (a) Marcus, R. A. *J. Chem. Phys.* **1956**, *24*, 966. (b) Marcus, R. A. *Discuss. Faraday Soc.* **1960**, *29*, 21. (c) Marcus, R. A. *J. Chem. Phys.* **1965**, *43*, 679.
(52) Griffiths, T. R.; Pugh, D. C. *Coord. Chem. Rev.* **1979**, *29*, 129.
(53) *Handbook of Chemistry and Physics*, 57th ed.; Chemical Rubber Publishing Co.: Cleveland, 1976.

infrared absorption bands, such as for water and for other hydroxylic solvents. Δ_s takes the following limiting forms in the high- and low-temperature limits where $\beta\hbar\omega \ll 1$ and $\beta\hbar\omega \gg 1$, respectively, for all ω

$$\Delta_s \rightarrow 2\sqrt{E_s k_B T} \text{ and } \Delta_s \rightarrow \sqrt{2E_s\hbar\omega_m} \qquad (10)$$

i.e., the band width is proportional to $T^{1/2}$ and independent of T, respectively.

Gaussian bands are obtained only near the absorption maximum. Deviations arise in the band wings, giving

$$K(\nu) = \frac{2\sqrt{\pi}}{\beta\Delta_s}\exp\left[-\frac{(h\nu - h\nu_m)^2}{\Delta_s^2} + \xi_3\frac{(h\nu - h\nu_m)^3}{\Delta_s^3} - \ldots\right] \qquad (11)$$

where ξ_3 is a positive coefficient. Its explicit form is given by the frequency dispersion, viz.[42]

$$\xi_3 = \frac{4}{3}\frac{\hbar^2}{\beta}\Delta_s^{-3}\int_0^{\omega_c} d\omega\ \omega f(\omega) \qquad (12)$$

The following general conclusion follows from eq 11. Since $\xi_3 > 1$, then $K(\nu)$ falls off more slowly on the high- than on the low-frequency side of the maximum. This "asymmetry" is more pronounced the lower the temperature and the higher the frequencies.

2. The Effect of Local Modes. Coupling to local nuclear potentials modifies the bandshape function to the following general form

$$K(\nu) = (Z_{qu}^{g})^{-1}\sum_v\sum_w S_{vw}K_s(h\nu + \epsilon_{ew} - \epsilon_{gv});$$
$$Z_{qu}^{g} = \sum_v \exp(-\beta\epsilon_{gv}) \qquad (13)$$

where S_{vw} is the local mode Franck Condon overlap factor involving the v'th and w'th vibrational wave functions in the ground and excited electronic state, respectively, ϵ_{gv} and ϵ_{ew} are the corresponding vibrational energies, and Z_{qu}^{g} is the local mode statistical sum in the ground electronic state. K_s is finally the $K(\nu)$ function for the solvent alone, the energy gap of each local mode vibronic component being modified by the appropriate level difference.

Franck–Condon factors for rather general nuclear potentials are available and impose additional band width, asymmetry, temperature, and vibrational fine-structure features. We provide here the following features of a single additional displaced harmonic nuclear mode of frequency Ω_c and (dimensionless) displacement Δ_c. The bandshape function is

$$K(\nu) = \frac{2\sqrt{\pi}}{\beta\Delta_s}\sum_{n=-\infty}^{n=\infty}\Phi_n\exp\left[-\frac{(h\nu - h\nu_m + n\hbar\Omega_c)^2}{\Delta_s^2}\right]$$
$$\Phi_n = I_{|n|}\left(\frac{\Delta_c^2}{sh(\frac{1}{2}\beta\hbar\Omega_c)}\right)\exp[\tfrac{1}{2}\beta\hbar\Omega_c - \tfrac{1}{2}\Delta_c^2\coth(\tfrac{1}{2}\beta\hbar\Omega_c)] \qquad (14)$$

where $I_{|n|}$ is the modified Bessel function of order $|n|$. The absorption spectrum thus now consists of an asymmetric envelope of Gaussian subbands, each of width Δ_s and separated by $\hbar\Omega_c$ We shall exploit this form in section IV. The bandshape can be brought to compacter forms for certain limits of the parameters. These forms are available elsewhere,[42] but we note presently that local mode vibrational fine-structure is smeared out for sufficiently wide solvent broadening, i.e., for $\Delta_s > \hbar\Omega_c$, the overall bandshape near the maximum becomes Gaussian and given by eq 3, the width and maximum energy, however, now being

$$\Delta_{tot} = [\Delta_s^2 + 2E_{rc}\hbar\Omega_c\coth(\tfrac{1}{2}\beta\hbar\Omega_c)]^{1/2};$$
$$h\nu_m = \Delta F_0 + E_s + E_{rc} \qquad (15)$$

where $E_{rc} = \frac{1}{2}\hbar\Omega_c\Delta_c^2$ is the local mode reorganization energy. The solvent and local modes thus contribute now "on equal footing" to the band width, cf. eq 4.

3. Environmental Nonequilibrium Polarization Modulation of the Electrtonic Transition Dipole Matrix Element. The formalism in eq 1–15 rests on a Condon scheme which implies that the absorption bandshape is dominated by the nuclear factor. The orbitals involved in the solvatochromic charge transfer transition are, however, strongly exposed to the environmental polarization fluctuations, and since the instantaneous solvent nuclear coordinates differ significantly from their equilibrium values, so will the transition dipole matrix element. This quantity must therefore also depend on the incoming light frequency, in principle leading to a distortion of the band relative to bandshapes with constant M_{eg}.

We have recently investigated both such environmental modulation effects and non-Condon effects on the electronic factor.[46,47] Explicit results are available for exponential single-parameter wave functions, including structureless as well as frequency dispersive solvents

$$\psi_g(\rho) = (\lambda_g^3/\pi)^{1/2}\exp(-\lambda_g|\vec{\rho}|);$$
$$\psi_e(\rho) = (\lambda_e^3/\pi)^{1/2}\exp(-\lambda_e|\vec{\rho} - \vec{R}|) \qquad (16)$$

where the orbital exponents in the ground (λ_g) and excited states (λ_e) are the only parameters; ρ are the electronic coordinates and R is the separation between the ground and excited state charge transfer centers. The crucial observation is now that the modulation effect leads the ground state wave function to expand on the low-frequency side of the absorption band maximum (lower λ_g) compared to its value at the equilibrium polarization, whereas it contracts on the high-frequency side (larger λ_e), and vice versa for the excited state orbital. Close to the maximum the following simple form of λ_g can reproduce the effects

$$\lambda_g(\theta^*) \approx \lambda_{go}\frac{(11/5) + (16z_D/5c\epsilon_s) - \xi\theta^*}{(11/5) + (16z_D/5c\xi_s)}; \qquad c = \epsilon_o^{-1} - \epsilon_s^{-1}$$

$$\xi = \frac{2}{\pi c}\int_0^\infty \frac{d\omega}{\omega}\frac{\mathrm{Im}\epsilon(\omega)}{|\epsilon(\omega)|^2}\frac{\frac{1}{2}\beta h\omega}{\tanh(\frac{1}{2}\beta h\omega)} \qquad (17)$$

where λ_{go} is the equilibrium value of λ_g, z_D is the "effective" donor core charge, and θ^* is the transfer coefficient ($\approx k_B T\ d\ \ln \kappa_{eg}(\nu)/d(h\nu)$) for the optical electronic process. λ_e is obtained from eq 17 by the transformations $\theta^* \rightarrow 1 - \theta^*$ and $z_D \rightarrow z_A$, z_A being the acceptor core charge. In the high-temperature limit and for vanishing core charges, i.e., when the electron is trapped solely by the inertial solvent polarization field, eq 17 takes the compact form

$$\lambda_g(\theta^*) \approx \lambda_{go}\left(1 - \frac{5}{11}\theta^*\right) \qquad (18)$$

Criteria for the importance of these effects compared with those of the nuclear factor were provided in ref 45–47. The dominating effect is a temperature-dependent red-shift of an otherwise largely undistorted band which appears when λ_e significantly exceeds λ_g, while a much smaller blue-shift and a weakly frequency dependent absolute absorption increase arises when $\lambda_g \gg \lambda_e$.

Modulation of the electronic wave functions and non-Condon effects can well be important for the solvatochromic betaine bands involving long-range electron transfer between solvent-exposed orbitals. The effects can, however, only be assessed more precisely by comparison between the corresponding absorption and emission bands. This would provide the appropriate values of ΔF_0 which would precisely illuminate the correspondence between the maximum and width of the bands (cf. ref 14).

IV. Bandshape Parameters for Betaine-26 in Different Solvents

Absorption spectra for betaine-26 were recorded for a wide range of different polar and apolar, and protic and aprotic solvents. In particular, the range of the solvent parameter c was far wider than what can be achieved for mixed-valence compounds. The solvatochromic band was always well isolated from other bands. This feature warranted bandshape analysis in some detail

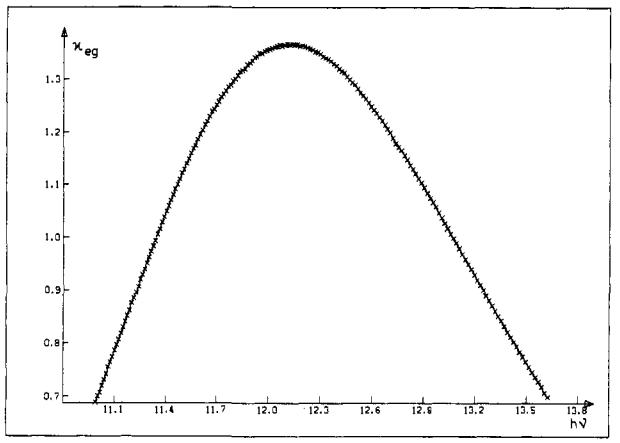

Figure 2. Example of fit of eq 14 to on-line data (betaine-26 in iodobenzene solution). The crosses indicate the experimental data points and the fully drawn line the least-squares fit of eq 14. The abscissa is the light frequency in units of 10^3 cm^{-1} and the ordinate the molar extinction coefficient in units of 10^4 dm^3 mol^{-1} cm^{-1}.

The bands are notably asymmetric, clearly with a slower fall-off on the high-frequency side (Figure 2). This is indicative of substantial coupling either to a molecular mode or to a high-frequency branch in the solvent dispersions. The former is understandable in view of the significant single-to-double-bond character change of the C–O bond in the phenolate ring or the interring C–N bond on excitation, as suggested by the scheme in Figure 1. Coupling to high-frequency solvent bands might also be expected for the hydroxylic solvents, but the asymmetry would vanish for aprotic solvents if this were the only coupling mode. Asymmetry clearly remains, however, for all the solvents, substantiating significant coupling to intramolecular coordinates.

The absorption band maximum varies from 587 nm for the most polar solvent accessible (methanol) to 907 nm for the most apolar one (carbon disulfide). For this latter and certain other apolar solvents, the solvent parameter $\epsilon_o^{-1} - \epsilon_s^{-1}$ in fact formally vanishes altogether.

The data for all the aprotic solvents could always be accurately represented by least-squares fitting of eq 14 and 15, regarding Δ_s, $\hbar\Omega_c$, Δ_c, M_{eg}, and $h\nu_m$ as parameters. An example of this, i.e., betaine-26 in iodobenzene, is shown in Figure 2. Of these parameters, Δ_s can be correlated with suitable solvent representations by means of the formalism in section III, while the constancy or solvent variation of Δ_c and $\hbar\Omega_c$ reveals the extent to which these two quantities are truly molecular quantitites. The maximum absorption energy, $h\nu_m$, has constituted the basis for the empirical E_T solvent polarity scale. However, $h\nu_m$ cannot be correlated with particular solvent representations in the same fashion as Δ_s, since it is determined by the two quantities E_s and ΔF_0 both of which vary with the solvent. There is no way of disentangling both quantities from the absorption spectrum alone except by the band width determination of E_s. This leaves a set of ΔF_0 values for which only the emission spectra of solute betaine-26 might provide independent checks.

The absolute molar absorbance values, for the hydroxylic solvents in particular, could vary by up to 10% as is also reported in ref 25–27. This only affected the pre-exponential part of eq 14 and 15 extracted from the data, but not the bandshape parameters Δ_s, $h\nu_m$, Δ_c, and Ω_c.

Figures 3–5 show the bandshape parameters extracted by means of eq 14 and 15, i.e. by regarding the bands as envelopes of Gaussian solvent sub-bands and the Franck–Condon terms of a single harmonic high-frequency mode. These figures reveal the following somewhat entangled picture.

(A) Non-hydroxylic, polar solvents indeed display a good correlation between the solvent band width, Δ_s, and $\epsilon_o^{-1} - \epsilon_s^{-1}$ as for a structureless solvent (cf. eq 4 and 8), in the range 0.48–0.73 for the latter. If acetone and tetrahydrofuran are exempted, the correlation is in fact almost "excellent". This is also the range covered by betaine-1[14] and by some intervalence transitions in

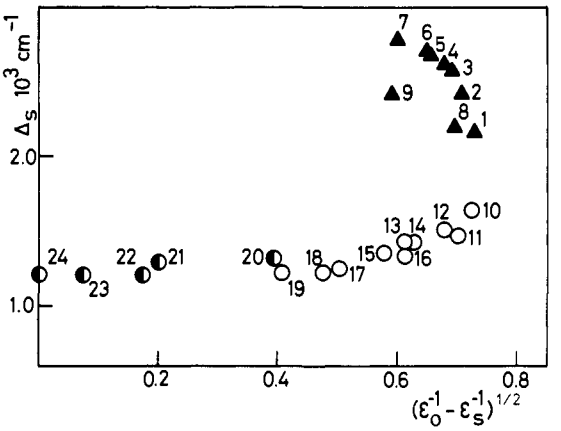

Figure 3. Solvent band widths, Δ_s, in units of 10^3 cm^{-1}, for the betaine-26 solvatochromic absorption band obtained by least-squares fits of eq 14 to the data, plotted against the solvent "polarity" parameter $(\epsilon_o^{-1} - \epsilon_s^{-1})^{1/2}$ ϵ_o is identified by the squared refractive index at the sodium D line, n_D. n_D and Δ_s data are from refs 52 and 53. The filled triangles represent alcohols, the open circles aprotic "polar" solvents, and the half-filled circles apolar aprotic solvents. The numbering is the same as in Table V.

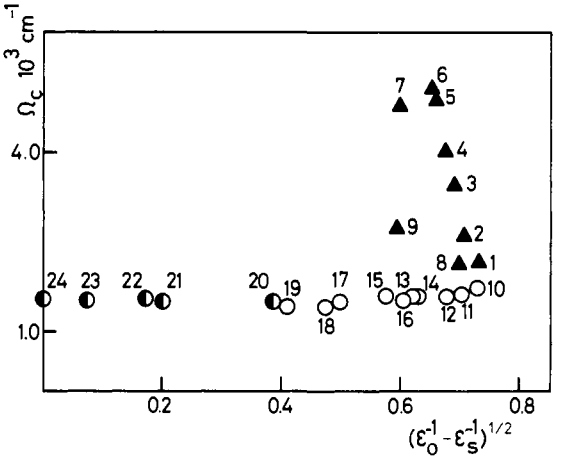

Figure 4. Dependence of the molecular vibrational frequency, Ω_c, in units of 10^3 cm^{-1}, on the solvent "polarity" parameter $(\epsilon_o^{-1} - \epsilon_s^{-1})^{1/2}$, obtained by least-squares fits of eq 14. Same numbering as in Figure 3 and Table V.

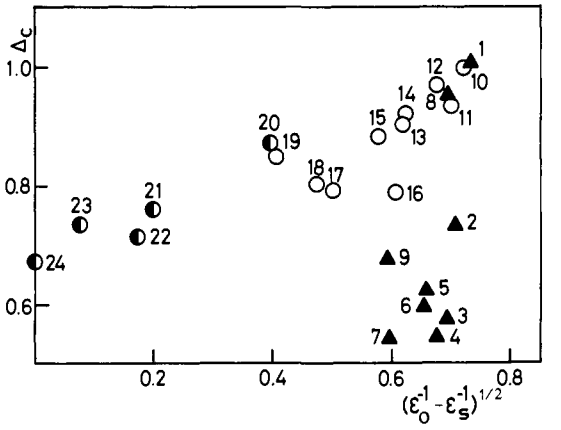

Figure 5. Dependence of the dimensionless equilibrium coordinate displacement Δ_c $(= (\mu\Omega_c/\hbar)^{1/2}\Delta R$, where ΔR is the real coordinate displacement in units of length and μ the effective mass associated with the molecular mode) on the solvent "polarity" parameter $(\epsilon_o^{-1} - \epsilon_s^{-1})^{1/2}$. Least-squares fit of the single-mode approximation, eq 14. Numbering is the same as in Figures 3 and 4 and in Table V.

mixed-valence compounds. The corresponding solvent reorganization free energies range from 0.22 to 0.40 eV, the correlation extrapolating to $E_s \approx 0.02$–0.03 eV, or a band width of 4–500

Table I. Betaine-26 Solvatochromic Absorption Bandshape Parameters Obtained by means of the Two Molecular Modes and Linear Solvent Approximation (eq 13, 14, and 19)[a]

solvent	Δ_s	$h\nu_m$	A	Ω_c	Δ_c
methanol	2.14 ± 0.05	262 ± 5	16.98 ± 0.05	2.4 ± 0.1	0.84 ± 0.04
ethanol	2.39 ± 0.05	372 ± 4	15.91 ± 0.05	2.9 ± 0.3	0.61 ± 0.05
1-propanol	2.54 ± 0.06	387 ± 9	15.57 ± 0.06	3.8 ± 0.9	0.52 ± 0.02
1-butanol	2.55 ± 0.05	416 ± 50	15.27 ± 0.04	4.9 ± 1.8	0.53 ± 0.22
benzonitrile	1.42 ± 0.02	1190 ± 10	12.77 ± 0.02	1.50 ± 0.09	0.60 ± 0.04

[a] Ω_c and Δ_c for one of the modes fixed at 1600 cm^{-1} and 0.7, respectively. Δ_s, $\hbar\nu_m$, and Ω_c in units of 10^3 cm^{-1}. $A = (8\pi^{5/2}/\ln 10)(\nu/c)|M_{eg}|^2/\Delta_s$ in units of dm^3 mol^{-1} cm^{-1}.

Table II. Betaine-26 Solvatochromic Absorption Bandshape Parameters Obtained by the Single-Mode Approximation (eq 14) [Units as in Table I]

solvent	Δ_s	$h\nu_m$	A	Ω_c	Δ_c
methanol	2.17 ± 0.05	17.06 ± 0.06	258 ± 5	2.2 ± 0.1	1.02 ± 0.05
ethanol	2.43 ± 0.05	16.01 ± 0.07	366 ± 5	2.7 ± 0.2	0.74 ± 0.06
1-propanol	2.58 ± 0.06	15.67 ± 0.07	379 ± 5	3.5 ± 0.8	0.58 ± 0.04
1-butanol	2.62 ± 0.07	15.44 ± 0.07	390 ± 20	4.1 ± 1.3	0.56 ± 0.05
1-hexanol	2.72 ± 0.05	15.09 ± 0.04	420 ± 60	5.1 ± 1.7	0.60 ± 0.2
1-decanol	2.79 ± 0.07	14.55 ± 0.06	470 ± 50	4.8 ± 1.9	0.55 ± 0.15
benzonitrile	1.42 ± 0.01	12.77 ± 0.02	1195 ± 10	1.56 ± 0.03	0.92 ± 0.02

cm^{-1}. This intercept is indicative of additional low-frequency molecular reorganization, possibly in torsional modes associated with the bulky *tert*-butyl substituents, but elusive of more precise identification. No intercept was obtained from band width analysis for betaine-1[14] which has no such substituents, but as noted, this outcome rested on the low-frequency part of the band only.

Apolar solvents, such as toluene or carbon disulfide with almost "abnormally" low $\epsilon_0^{-1} - \epsilon_s^{-1}$ do not fit the correlation. The band width is larger and rapidly turns into a constant value for $\epsilon_0^{-1} - \epsilon_s^{-1}$ lower than about 0.4, corresponding to a solvent reorganization free energy of about 0.2 eV. Strong solute–solvent coupling thus appears to remain for apolar aprotic solvents. The nature of this coupling cannot be long-range electrostatic interaction, but it could be induced by multipolar or dispersion forces, or by pressure-density or pseudo-potential-like[54] forces from the solvent environment to which a spatially more voluminous excited state wave function would be exposed. Such effects are encountered for metal atoms trapped in noble gas matrices[55] (cf. discussion in ref 42).

The solvent band width for the normal alcohols and some other hydrogen bonding solvents is about twice as large as that for the most polar aprotic solvents, i.e., $\Delta_s \approx 0.3$ eV or $E_s \approx 0.9$ eV. A single-mode representation, however, gave poorer fits to the data than for the polar aprotic solvents, and the values do not in any way exhibit the correlation with $\epsilon_0^{-1} - \epsilon_s^{-1}$ expected for a structureless dielectric. Both observations are likely to be caused by hydrogen bond formation to the phenolate group, in spite of extensive expected screening by the bulky *tert*-butyl groups (cf. discussion in ref 26). There is a tendency that Δ_s for the normal alcohols increases with increasing molecular weight, but this effect vanishes except for 1-hexanol and 1-decanol when the modified fitting procedure, outlined under point B below, is used. Since the measurements refer to vibrationally equilibrated systems, viscosity and "frictional" origins[56] of a molecular weight dependence can be ruled out, and the molecular weight variation of Δ_s rather reflects increasing hydrogen bond strength induced by the hydrophobic parts of the solvent molecules.[57,58] Attemps to verify this distinction by spectral recording for trifluoro- and trichloroethanol solvents unfortunately failed due to decomposition of betaine-26 in these solvents.

tert-Amyl alcohol does not follow the same pattern as for the normal alcohols, but rather it follows the one for aprotic polar solvents. This could be caused by disruption of the hydrogen bond structure induced by structural incompatibility with the methyl substituents in the molecules of this solvent.

(B) Figure 4 shows the molecular vibrational frequencies. For all the aprotic solvents these values have been obtained by least-squares fitting of eq 14 to the data. Most striking is the remarkable constancy for all, polar and apolar, protic solvents. The value is 15–1600 cm^{-1} which is close to what is expected for aromatic ring skeletal modes or the C–O and C–N bonds reorganized on excitation (Figure 1). This emphasizes the nature of this mode as a molecular mode.

The frequencies are much higher for the alcohols, ranging from 22 to 2600 cm^{-1} for methanol and ethanol to twice this value for the heaviest alcohols. The former values are in line with expectations if reorganization in hydrogen-bonded O–H stretch modes is important. On the other hand, the larger values reveal that the single-mode model is a poor representation, at least for the heavier alcohols. This would be understandable if there is a certain distribution of hydrogen bond modes caused by the disordered nature of the environments. The poor representation is also emphasized by the substantially larger variances for the parameters Δ_c and Ω_c for the alcohols compared with the aprotic solvents, whereas a small variance is still associated with Δ_s, also for the alcohols (cf. the tables below).

In order to illuminate this further, the single-mode procedure, resting on fitting eq 14 to the data and adequate for the aprotic solvents in the sense of giving low parameter variances, was modified to handle the alcohol data. Equation 14 was first converted to the corresponding form for two, rather than a single, molecular modes.[42,59] This equation has the form

$$K(\nu) = \frac{2\sqrt{\pi}}{\beta\Delta_s} \sum_{n_1=-\infty}^{\infty} \Phi_{n_1} \times \sum_{n_2=-\infty}^{\infty} \Phi_{n_2} \exp\left[-\frac{(h\nu - h\nu_m + n_1\hbar\Omega_{c1} + n_2\hbar\Omega_{c2})^2}{\Delta_s^2} \right] \quad (19)$$

where each of the subscripts "1" and "2" refer to one of the molecular degress of freedom, and Φ_{n_1} and Φ_{n_2} have the same form as in eq 14. Equation 19 is essentially a fourfold summation over the vibrational quantum numbers of each mode in both the initial and final states, but in practice only a few terms contribute.

One of the modes is now representative of the same truly molecular mode which emerged for the aprotic solvents and was associated with the (practically constant) values of Ω_c and Δ_c for these solvents, viz., $\Omega_c \approx 1600$ cm^{-1} and $\Delta_c \approx 0.7$ (cf. Figure 5 and point C below). Ω_c and Δ_c for the other one were regarded as parameters and allowed to vary in the minimization process.

(54) (a) Bardeen, J.; Schockley, W. *Phys. Rev.* **1950**, *77*, 407; 1953, *80*, 72.
(55) Weinert, C. M.; Forstmann, F.; Abe, H.; Grinter, R.; Kolb, D. M. *J. Chem. Phys.* **1982**, *77*, 3392.
(56) Frauenfelder, H.; Wolynes, P. G. *Science* **1985**, *228*, 337.
(57) Symons, M. C. R. In *Electron–Solvent and Anion–Solvent Interactions*; Kevan, L., Webster, B. C., Eds.; Elsevier: Amsterdam, 1976; p 311.
(58) Huot, J.-Y.; Jolicoeur, C. In *The Chemical Physics of Solvation*, Part A; Dogonadze, R. R., Kálmán, E., Kornyshev, A. A., Ulstrup, J. Eds.; Elsevier: Amsterdam, 1985; p 417.
(59) Itskovitch, E. M.; Vorotyntsev, M. A. *Opt. Spektros.* **1978**, *45*, 240.

Table III. Betaine-26 Solvatochromic Absorption Bandshape Parameters Obtained by Inclusion of Both Two Molecular Modes and a "Linear" Solvent with a High-Frequency Vibrational "Tail" (eq 11, 13, 14, and 19)[a]

solvent	Δ_s	A	$h\nu_m$	Ω_c	Δ_c	ξ_3
methanol	2.4 ± 0.3	220 ± 20	17.0 ± 0.6	1.7 ± 0.8	0.7 ± 0.5	−0.23 ± 0.03
ethanol	2.17 ± 0.07	404 ± 9	15.70 ± 0.06	2.1 ± 0.1	0.96 ± 0.08	0.13 ± 0.04
1-propanol	2.14 ± 0.03	434 ± 4	15.20 ± 0.03	1.91 ± 0.06	1.02 ± 0.02	0.215 ± 0.005
1-butanol	2.16 ± 0.04	445 ± 5	14.96 ± 0.04	1.90 ± 0.08	0.99 ± 0.05	0.220 ± 0.006
1-hexanol	2.31 ± 0.07	443 ± 8	14.68 ± 0.07	2.1 ± 0.2	0.86 ± 0.08	0.29 ± 0.02
1-decanol	2.47 ± 0.05	490 ± 10	14.15	2.3 ± 0.1	0.77 ± 0.06	0.12 ± 0.06
benzonitrile	1.49 ± 0.08	1130 ± 70	12.84 ± 0.07	1.8 ± 0.3	0.62 ± 0.17	−0.06 ± 0.06

[a] Ω_c and Δ_c for one mode fixed at 1600 cm^{-1} and 0.7, respectively. Units as in Tables I and II. Value of $h\nu_m$ for dodecanol fixed at 14.15 ± 10′ cm^{-1}.

Table IV. Comparison of Solvatochromic Absorption Bandshape Parameters for Betaine-26 in Methanol and O-Deuteriated Methanol (Same Model and Units as in Table I)

solvent	Δ_s	$h\nu_m$	A	Ω_c	Δ_c
methanol	2.14 ± 0.05	16.98 ± 0.05	262 ± 5	2.4 ± 0.1	0.84 ± 0.04
methanol-*O-d*	2.10 ± 0.05	16.88 ± 0.04	311 ± 5	2.2 ± 0.1	0.88 ± 0.04

The results for the four lightest alcohols are shown in Table I. In comparison, the numerical results of the fitting of the single-mode approximation are shown in Table II. It is obvious that inclusion of two discrete molecular modes leads to no improvement, neither in accuracy nor in the closer approach of the molecular parameters to expected real physical values. The results for a representative aprotic polar solvent, viz., benzonitrile, are also shown in the tables. The only difference for this solvent between the single- and two-mode approximations is apparently that Δ_c is smaller for the latter, since the molecular reorganization is here distributed among two nuclear coordinates.

Table III shows the results when a distribution of high-frequency modes rather than a single mode or two discrete modes are included, in addition to the two already present. The distribution is reflected by a finite value of the coefficient ξ_3 to the cubic term in the exponent of eq 11. With the exception of methanol and decanol this in fact does lead to significant improvements. The Ω_c values are now all in the range 19–2200 cm^{-1}, with little systematic variation, and all the parameters have low variances and positive values of ξ_3. The frequency values are, however, lower than those for even strongly hydrogen-bonded O–H stretching modes and may reflect a considerable bending or librational intermixing, if regarded literally as a single mode.

The value of ξ_3 is a measure of the contribution of a high-frequency solvent vibrational spectral "tail" to the broadening. The larger such a contribution is the larger also is the numerical value of ξ_3. For example, if the solvent dispersion can be regarded approximately as consisting of a low-frequency (classical) dominating band separated from a narrow high-frequency band centered at the frequency ω_q, then only the latter contribute to ξ_3, and it can be shown that ξ_3 is approximately $\xi_3 \approx {}^4/_3\Delta_s^{-3}(\hbar\omega_q)^2E_s^q$, where E_s^q is the reorganization free energy of the high-frequency band solvent modes. The ξ_3 values extracted from the bandshape analysis are in the range 0.1–0.2 from which the combination $(\hbar\omega_q)^2E_s^q$, but not $\hbar\omega_q$ and E_s^q separately, can be obtained. Identification of the high-frequency band tail with librational (800 cm^{-1}), O–H bending (1600 cm^{-1}), and O–H stretching (3000 cm^{-1}) modes would then give $E_s^q \approx 0.12$–0.25, 0.02–0.04, and 0.01–0.02 eV, respectively. This is to be compared with the overall E_s from the main band which is about 0.6 eV for the alcohols.

Methanol which was well approximated by both the single- and two-mode models is apparently poorly represented when finite values of ξ_3 are invoked. ξ_3 takes "unphysical" negative values, and the variances of Δ_s, Ω_c, and Δ_c become unacceptably high. No minimum could be found for decanol, but a good fit for reasonable parameter values was obtained when $h\nu_m$ was fixed at a value of 14.15 × 10^3 cm^{-1}, this value being chosen by inspection of the apparent variation of $h\nu_m$ for the other alcohols when the additional parameter ξ_3 is introduced.

(C) The coordinate shifts of the single-mode fits, Δ_c, are shown in Figure 5. The different solvent classes seem to be reflected in this quantity in a less-clearcut fashion. Aprotic solvents, including polar as well as apolar ones, seem to display a slight increase with increasing solvent polarity parameter. This could be indicative of some coupling between the local mode and the solvent. The variation is, however, much weaker than that for the solvent broadening Δ_s, and in view of the remarkable constancy of Ω_c for these solvents, the variation perhaps in the end rather reflects little more than scatter.

Within the single-mode approximation, the alcohols appear to give lower values than the aprotic solvents. However, this reflects the inadequacy of this model. When the multimode representation is used, Δ_c in fact adopts values in the range 0.8–1.0, and with a tendency of decreasing with increasing molecular weight of the alcohol.

The actual values of Δ_c are in the range 0.7–1.0 for the aprotic solvents, corresponding to a molecular reorganization energy E_{rc} of 0.1–0.15 eV. E_{rc} is higher for the alcohols, i.e., 0.2–0.25 eV, which emerges from Δ_c values of 0.8–1.0. If the molecular reorganization for the aprotic solvents were solely associated with the conversion of the C–O phenolate bond from a single bond to a quinoid bond-like state, this would correspond to a bond length change of 0.03–0.05 Å. This is quite a lot smaller than the real difference between single and double C–O bonds, so that the scheme in Figure 1 would only qualitatively represent the real structural reorganization with the excitation.

The Δ_c values for the alcohols would correspond to an equilibrium bond displacement of about 0.15 Å if associated solely with motion of a single hydrogen-bonded proton. This appears quite reasonable, but it must be viewed on the background of the likely "mixed-mode" character of this degree of freedom.

In order to illuminate the character of the local mode, the spectrum of betaine-26 in O-deuteriated methanol was recorded and compared with the spectrum for normal methanol. The parameters were extracted by means of the two-mode approximation without additional solvent band asymmetry (i.e., omitting the parameter ξ_3). The extracted parameter values are collected in Table IV. They do reveal that the deuterium isotope effect, although giving a smaller Ω_c and larger Δ_c for the deuteriated than for the protonated solvent as expected if hydrogen motion is involved, is still much smaller than that corresponding to the frequency ratio and in fact only slightly exceeds the accuracy in the parameters. The most straightforward explanation of this is that the molecular mode does not represent pure proton motion but also a significant element of solvent molecular libration.

Table V finally summarizes the parameters from the spectral data for all the solvents. These values are obtained by the different fitting procedures for the various solvents, reflecting the different physical properties of the solvents, such as noted above. The values in Table V are thus what is to be regarded as the "best" values consistent with the spectral data for the betaine-26 solvatochromic charge transfer absorption band, within the linear solvent and harmonic molecular mode approximations.

Table V. "Best" Values of Solvatochromic Absorption Bandshape Parameters for Betaine-26[c]

no.	solvent	$\sqrt{c}$	Δ_s	$h\nu_m$	A	Ω_c	Δ_c	ξ_3
1	methanol	0.732	2.14 ± 0.05	16.98 ± 0.05	262	2.4 ± 0.1	0.84 ± 0.04	
2	ethanol	0.706	2.17 ± 0.07	15.70 ± 0.06	404	2.1 ± 0.1	0.96 ± 0.08	0.13 ± 0.04
3	1-propanol	0.687	2.14 ± 0.03	15.20 ± 0.03	434	1.91 ± 0.06	1.02 ± 0.04	0.215 ± 0.005
4	1-butanol	0.674	2.16 ± 0.04	14.96 ± 0.04	445	1.90 ± 0.08	0.99 ± 0.05	0.220 ± 0.006
5	1-pentanol	0.657	2.67 ± 0.06	15.29 ± 0.05	432			
6	1-hexanol	0.650	2.31 ± 0.07	14.68 ± 0.07	443	2.1 ± 0.1	0.86 ± 0.08	0.29 ± 0.02
7	1-decanol	0.595	2.47 ± 0.05	14.15	490	2.3 ± 0.3	0.77 ± 0.06	0.12 ± 0.07
8	*N*-methylformamide	0.694	2.20 ± 0.05	16.32 ± 0.04	287	2.15 ± 0.07	0.96 ± 0.04	
9	benzyl alcohol	0.590	2.42 ± 0.06	15.95 ± 0.08	319	2.8 ± 0.4	0.70 ± 0.04	
10	acetonitrile	0.726	1.66 ± 0.02	13.79 ± 0.03	712	1.70 ± 0.04	1.00 ± 0.03	
11	acetone	0.702	1.49 ± 0.01	12.88 ± 0.02	993	1.63 ± 0.03	0.94 ± 0.02	
12	dimethylformamide	0.679	1.52 ± 0.04	13.28 ± 0.04	816	1.62 ± 0.07	0.97 ± 0.04	
13	nitrobenzene	0.620	1.43 ± 0.01	12.76 ± 0.01	1163	1.60 ± 0.03	0.91 ± 0.02	
14	benzonitrile	0.623	1.42 ± 0.01	12.77 ± 0.02	1195	1.56 ± 0.03	0.92 ± 0.02	
15	*tert*-amyl alcohol	0.578	1.36 ± 0.01	12.51 ± 0.01	523	1.63 ± 0.03	0.89 ± 0.01	
16	tetrahydrofuran	0.611	1.32 ± 0.01	12.08 ± 0.02	1572	1.54 ± 0.05	0.79 ± 0.02	
17	chlorobenzene	0.502	1.25 ± 0.01	11.93 ± 0.01	1445	1.50 ± 0.04	0.80 ± 0.02	
18	bromobenzene	0.475	1.24 ± 0.01	11.91 ± 0.01	1631	1.47 ± 0.04	0.80 ± 0.02	
19	iodobenzene	0.406	1.23 ± 0.01	11.87 ± 0.01	1469	1.43 ± 0.04	0.85 ± 0.02	
20	methylmetacrylate	0.394	1.33 ± 0.01	12.20 ± 0.02	1420	1.52 ± 0.04	0.87 ± 0.02	
21	dioxane	0.199	1.29 ± 0.01	11.80 ± 0.02	987	1.53 ± 0.06	0.76 ± 0.02	
22	toluene	0.173	1.21 ± 0.04	11.40 ± 0.04	1891	1.6 ± 0.3	0.72 ± 0.04	
23	benzene	0.072	1.22 ± 0.01	11.53 ± 0.02	2183	1.56 ± 0.08	0.74 ± 0.02	
24	carbon disulfide[b]		1.22 ± 0.02	1.02 ± 0.02	1523	1.6 ± 0.1	0.68 ± 0.02	

[a] Only calculated for the single-mode, Gaussian solvent model. [b] The value of $\epsilon_o^{-1} - \epsilon_s^{-1}$ for carbon disulfide is formally negative. [c] For methanol values are based on the two-mode model and a linear solvent with high-frequency "tail" (eq 13, 14, and 19). For other alcohols an additional solvent high-frequency tail is included (eq 11). Values for other solvents rest on the single-mode and classical solvent approximations (eq 14). $c = \epsilon_o^{-1} - \epsilon_s^{-1}$ from ref 52 and 53.

5. Discussion

Bandshape analysis of the solvatochromic charge transfer bands of betaines by means of multiphonon charge transfer theory which incorporates in principle all the dynamic features of both the solute molecular structure and the solvent has not previously been reported. Band maximum variation with the solvent has constituted the basis for empirical solvent polarity rationalization in terms of the E_T scale.[26-28,60] While the practical value of this is indisputable, multiphonon bandshape analysis, including in principle both vibrational frequency and spatial solvent dispersion,[24,35] offers to endow the solvatochromic band features with a more rigorous theoretical frame.

Betaines, and perhaps betaine-26 in particular, are suitable for illumination of the detailed bandshape properties, as a reflection of both molecular structural changes and strong solute–solvent interactions. This observation rests on the following solvatochromic bandshape properties:

(a) The solvatochromic band is well isolated from other electronic absorption bands (cf. ref 26), warranting altogether the detailed bandshape analysis.

(b) The charge transfer molecules readily dissolve in wide ranges of solvents with quite diversified properties. The range of solvents, for example, by far exceeds the range accessible to investigations of intervalence transitions in binuclear mixed-valence transition metal complexes which have occupied a prominent role in the evolution of charge transfer concepts.

(c) Not only the apparent and the real band maximum but also the band width and shape display characteristic variations with the solvent. Adequate band feature analysis of the former effect requires insight into both the solute–solvent coupling parameters and the free energy gap between the ground and excited electronic states. This could only be obtained by comparative analysis of absorption and emission band profiles. Such a comparison would also illuminate the extent to which environmental modulation of the transition dipole matrix element[45-47] and non-Condon effects are important (cf. section III.3). On the other hand, shape features can be given a theoretical frame in terms of multiphonon bandshape theory on the basis of absorption band data alone.

(d) The betaine-26 bands are notably asymmetric with a slower fall-off on the high-frequency side of the maximum. The appearance of asymmetry in all the solvents and not merely in the ones with an expected vibrational high-frequency "tail" in the dispersion (the normal alcohols) is indicative that it originates from reorganization in the molecular structure itself.

We have exploited these features of the betaine-26 solvatochromic charge transfer band to extract the appropriate molecular and solvent coupling parameters by charge transfer bandshape theory, for a range of protic and aprotic solvents, and to investigate the variation of the coupling parameters with the nature of the solvents. The results can be summarized in the following points:

(1) The broad, asymmetric band can indeed be accurately reproduced by the asymmetric envelopes of Gaussian or cubic-exponential sub-bands which emerge from solute molecular bandshape theory[42] when coupling to both the solvent and to intramolecular degrees of freedom is important.

(2) The "best" specific bandshape expressions are, however, different for the different classes of solvents investigated. The simplest form is, not surprisingly, obtained for aprotic solvents. The bands are here accurately reproduced by an asymmetric envelope of Gaussian sub-bands and the Franck–Condon terms of a single molecular degree of freedom. The molecular nature of the latter is strikingly corroborated by the virtual constancy of about 1600 cm^{-1} of the vibrational frequency of this mode for a very wide range of the dynamic solvent polarity parameter $\epsilon_o^{-1} - \epsilon_s^{-1}$. This value is close to expectations for C–C, C–N, or C–O stretching modes likely to be the ones displaced on photoexcitation. The corresponding displacements exhibit more variation, but still substantially less than the solvent coupling itself, and are most likely indistinguishable from scatter.

(3) The Gaussian sub-bandwidth Δ_s for the aprotic solvents displays a different pattern for polar and apolar solvents. Δ_s for polar solvents is well correlated with $\epsilon_o^{-1} - \epsilon_s^{-1}$ over the same range of the latter as when such correlations have been reported for the band maxima of intervalence transitions in binuclear transition metal complexes. A structureless dielectric solvent approximation and long-range bulk solute–solvent electrostatic coupling adequately reproduce this feature. Δ_s for lower values of $\epsilon_o^{-1} - \epsilon_s^{-1}$ is approximately constant, indicative of other kinds of solute–solvent interaction forces, such as multipole, pressure–density, and pseudopotential interactions.

Protic solvents, here represented by a range of normal aliphatic alcohols, exhibit a different kind of bandshape pattern, most likely originating from hydrogen bond and other specific solute–solvent

(60) Reichardt, C.; Harbusch-Görnert, E. *Ann. Chem.* **1983**, 721.

interactions. More precisely this can be summarized in the following way:

(4) Methanol differs in this respect from the heavier alcohols. The bandshape for betaine-26 in methanol is only well reproduced if two, rather than a single, molecular modes are introduced into the bandshape expressions and combined with Gaussian solvent-broadened sub-bands. If one of the two modes is associated with the same degree of freedom as emerged for the aprotic solvents, then the vibrational frequency and displacement values of the second one, i.e., 2400 cm^{-1} and 0.84, respectively, are indicative that O-H stretching and bending are involved in the reorganization of this mode. This is, however, only partly borne out by the deuterium isotope effect investigations. Although the appropriate frequency is smaller and the displacement larger for the deuteriated methanol, as expected when O-H reorganizations are involved, the emerging frequency ratio is smaller than the ratio between pure O-H frequencies. This suggests that the second molecular mode for methanol contains elements of librational motion which are much less isotope sensitive.

The remaining solvent band broadening, Δ_s, does not fit the $\epsilon_0^{-1} - \epsilon_s^{-1}$ correlation for the polar solvents but is larger by 10-15%. This observation is also indicative of some additional, either vibrational or spatial, solvent dispersion, but so far it is elusive of more precise identification.

(5) Solvent vibrational dispersion appears even more pronounced for the heavier alcohols, for which the two-mode Gaussian approximation is also inadequate. Accurate band representation is, however, obtained if the additional asymmetry parameter ξ_3 is introduced. The parameters for the two molecular modes which emerge for the heavier alcohols then coincide approximately with the ones for methanol, while the asymmetry of the sub-bands and the relatively large values of Δ_s must reflect additional high-frequency solvent dispersion which is not well incorporated by a discrete single-mode approximation.

We can conclude that rigorous bandshape analysis for betaine-26 has provided physically plausible and quite precise criteria for the adequacy or failure of the simplest approach to solute-solvent interactions as bulk electrostatic coupling to a structureless dielectric. It has also provided a disclosure of the nature of the solute intramolecular reorganization which accompanies the electronic transition. Such achievements furthermore have to rely on bandshape rather than band maximum analysis. A clue to the more composite behavior of protic solvents has finally emerged. Specific interactions, the nature of which can be traced to hydrogen bonding, perhaps solvent librational motion, and dispersion in the solvent vibrational frequency spectrum, can thus account for nearly all the observed band features for these solvents. Further details of this could be substantiated by suitable molecular models for the solvent and the solute-solvent interactions. As disclosed by our present analysis, the formalism applied here has the merit of incorporating such solvent structural details in the form of vibrational frequency and spatial dispersion of the solvent susceptibility functions, thus going far beyond structureless continuum models. Such a requirement is also needed in the elucidation of real solute-solvent interactions.

Acknowledgment. We acknowledge financial support from the Danish Natural Science Research Council.

Laser Flash Photolysis Studies of Methoxycarbonyl Phenyl Carbene and Its Derived Carbonyl Oxide at Room Temperature

Yoshihisa Fujiwara,[1a] Yoshifumi Tanimoto,[1a] Michiya Itoh,*[1a] Katsuyuki Hirai,[1b] and Hideo Tomioka[1b]

Contribution from the Faculty of Pharmaceutical Sciences, Kanazawa University, Takara-machi, Kanazawa 920, Japan, and the Department of Industrial Chemistry, Faculty of Engineering, Mie University, Tsu, Mie 514, Japan. *Received August 25, 1986*

Abstract: Laser flash photolysis of methyl α-diazophenylacetate gives triplet methoxycarbonyl phenyl carbene (^{3}MPC) exhibiting a transient absorption spectrum (<270 nm), which shows a pseudo-first-order decay with lifetime of 461 ns in deaerated Freon 113. The triplet carbene readily reacts with an oxygen molecule to afford a corresponding carbonyl oxide in aerated solvents at room temperature. The formation of carbonyl oxide was demonstrated by the buildup of the transient absorption spectrum ($\lambda_{max} \sim 410$ nm) at the expense of the absorption band of the carbene. Quenching rate constants of this triplet carbene by 2-methyl-2-butene and methyl alcohol were obtained to be 7.0×10^7 M^{-1} s^{-1} and 2.7×10^8 M^{-1} s^{-1}, respectively, by means of monitoring the decay of the triplet carbene. The difference of the reactivity between the triplet carbene and the carbonyl oxide toward methyl alcohol has been investigated. The carbonyl oxide is much more stable with methanol than the parent triplet carbene (^{3}MPC). Kinetic data reported in this paper demonstrate that the stability of this carbene (^{3}MPC) is regarded as an intermediate between reported diphenylcarbene and fluorenylidene.

It is well-known that an oxygen molecule scavenges a triplet carbene[2-5] to afford an intermediate, carbonyl oxide, which is ultimately led to the formation of a corresponding ketonic compound. Recently, aromatic carbonyl oxides, which are frequently refered to as Criegee intermediates,[6] have been studied by means of laser flash photolysis in organic solvents at room temperature.[7-10] Scaiano and his co-workers[8,9] have reported a transient absorption spectrum of a carbonyl oxide formed from triplet diphenylcarbene and oxygen, and also they[11] have presented information about the

(1) (a) Kanazawa University. (b) Mie University.
(2) Bartlett, P. D.; Traylor, T. G. *J. Am. Chem. Soc.* **1962**, *84*, 3408.
(3) Trozzolo, A. M. *Acc. Chem. Res.* **1968**, *1*, 329.
(4) Murray, R. W.; Suzui, A. *J. Am. Chem. Soc.* **1971**, *93*, 4963.
(5) Closs, G. L.; Rabinow, B. E. *J. Am. Chem. Soc.* **1976**, *98*, 8190.
(6) (a) Criegee, R. *Rec. Chem. Prog.* **1957**, *18*, 111. (b) Criegee, R. *Angew. Chem., Int. Ed. Engl.* **1975**, *14*, 745.
(7) Sugawara, T.; Iwamura, H.; Hayashi, H.; Sekiguchi, A.; Ando, W.; Liu, M. T. H. *Chem. Lett.* **1983**, 1261.
(8) Werstiuk, N. H.; Casal, H. L.; Scaiano, J. C. *Can. J. Chem.* **1984**, *62*, 2391.
(9) Casal, H. L.; Sugamori, S. E.; Scaiano, J. C. *J. Am. Chem. Soc.* **1984**, *106*, 7623.
(10) Casal, H. L.; Tanner, M.; Werstiuk, N. H.; Scaiano, J. C. *J. Am. Chem. Soc.* **1985**, *107*, 4616.

0002-7863/87/1509-1942$01.50/0